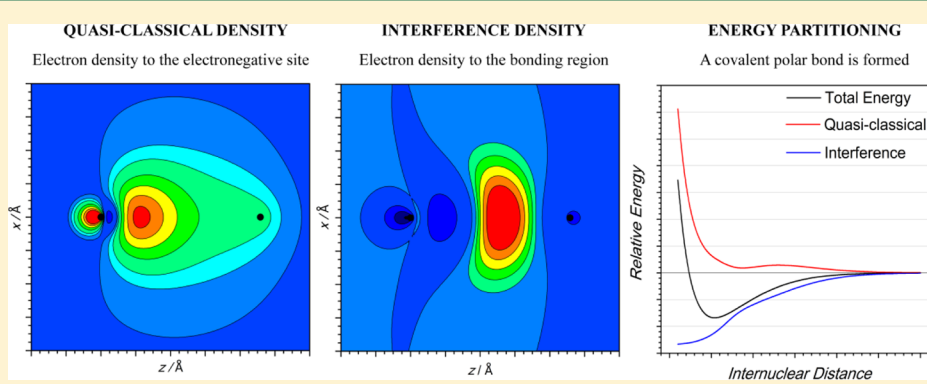


# Description of Polar Chemical Bonds from the Quantum Mechanical Interference Perspective

Felipe Fantuzzi and Marco Antonio Chaer Nascimento\*

Instituto de Química, Universidade Federal do Rio de Janeiro, Rio de Janeiro, RJ 21941-909, Brazil



**ABSTRACT:** The Generalized Product Function Energy Partitioning (GPF-EP) method has been applied to a set of molecules, AH ( $A = Li, Be, B, C, N, O, F$ ), CO and LiF with quite different dipole moments, in order to investigate the role played by the quantum interference effect in the formation of polar chemical bonds. The calculations were carried out with GPF wave functions treating all the core electrons as a single Hartree–Fock group and the bonding electrons at the Generalized Valence Bond Perfect-Pairing (GVB-PP) level, with the cc-pVTZ basis set. The results of the energy partitioning into interference and quasi-classical contributions along the respective Potential Energy Surfaces (PES) show that the main contribution to the depth of the potential wells comes from the interference term, which is an indication that all the molecules mentioned above form typical covalent bonds. In all cases, the stabilization promoted by the interference term comes from the kinetic contribution, in agreement with previous results. The analysis of the effect of quantum interference on the electron density reveals that while polarization effects (quasi-classical) tend to displace electronic density from the most polarizable atom toward the less polarizable one, interference (quantum effects) counteracts by displacing electronic density to the bond region, giving rise to the right electronic density and dipole moment.

## 1. INTRODUCTION

Chemical bond is usually considered to be a very well established concept in chemistry. Nevertheless, its origin and nature are still subject to much discussion and scientific inquiry.<sup>1–25</sup> In spite of the fact that the minimum in the potential energy surface (PES) responsible for the bond in a stable system is followed by a decrease of potential energy and a rise of kinetic energy, as required by the virial theorem, this type of analysis does not provide a model for explaining bond formation. Since the total kinetic and potential energies are a direct consequence of the form of the total electronic density, the question of why the electronic density of a bonded molecule changes in such a way that results in an energy drop is unanswered by these quantities.<sup>1–3</sup> It is possible to understand the reason why chemical bonds are formed by means of an alternative energy partitioning, derived from a density partitioning, in quasi-classical and interference contributions.<sup>1,4,5</sup> This approach shows that the quantum mechanical interference effect promotes a change in the electron density which is responsible for the energy reduction that leads to the formation of covalent bonds. The results obtained for a variety of diatomic and polyatomic molecules based on this kind of energy

partitioning attest that such bonds are formed only in the presence of quantum interference.<sup>1–10</sup>

In previous papers, we developed an energy partition scheme, known as the Generalized Product Function Energy Partitioning Method (GPF-EP), and used it to investigate the chemical bond in different classes of molecules,<sup>5–10</sup> including a range of homonuclear (AA) bonds<sup>5,6</sup> in diatomic and polyatomic molecules.<sup>7–10</sup> According to this approach, detailed in section 2, the total energy of the molecule is partitioned into a contribution due to the quantum interference effect and a contribution due to all the other effects, collectively referred as to quasi-classical or reference contribution.

The molecules previously studied<sup>2–10</sup> are all made of nonpolar or slightly polar bonds, and for these molecules the central role played by the interference energy can be easily verified to be determinant for the formation of each one of the bonds. Normally, nonpolar or slightly polar bonds are considered to be “covalent” bonds but this sort of association can lead to the unjustified conclusion that quantum

Received: February 8, 2014



interference only plays a dominant role in the formation of nonpolar or slightly polar bonds and, even worse, that polar bonds are predominantly noncovalent and that highly polar bonds are essentially “ionic”.

In order to show that there is no direct relation between the quantum mechanical interference contribution to the formation of a chemical bond and its polarity, we propose to examine the interference energy in diatomic molecules, AB, presenting different polarities. This can be accomplished by selecting different pairs of distinct A and B atoms or by fixing one of them and varying the other, as to scan a reasonable range of values of dipole moments. For a comparative analysis the second choice is more convenient and the series of molecules A-H, with A = Li, Be, B, C, N, O, and F provides an excellent test, inasmuch as the dipole moment not only varies gradually in magnitude but also changes its sign as one moves from lithium hydride ( $\mu = -5.88$  D) to hydrogen fluoride ( $\mu = 1.82$  D). In addition, from all AB (A, B  $\neq$  H) molecules that can be formed with the first row elements, we also considered LiF and CO because they represent two excellent tests for the theory. According to any simple qualitative or semiquantitative analysis based on pure electrostatic models, LiF, being formed from atoms occupying the two extreme positions in the periodic table, should be the most “ionic” of the bonds, while CO should be less ionic but exhibiting a dipole moment with the negative end at the O atom, contrary to the experimental observations.

## 2. PARTITIONING OF THE INTERFERENCE ENERGY AND DENSITY

The method for energy partitioning used herein is called Generalized Product Function Energy Partitioning (GPF-EP)<sup>5</sup> and was derived by applying Ruedenberg's<sup>4</sup> original partitioning scheme to GPF wave functions constructed with Modern Valence Bond group functions. The GPF wave functions have been defined by McWeeny, and their general form is shown in eq 1:

$$\Psi_{\text{GPF}} = \hat{A}\{\Psi_1(\vec{r}_1\vec{\omega}_1, \vec{r}_2\vec{\omega}_2, \dots, \vec{r}_{N_1}\vec{\omega}_{N_1})\Psi_2 \\ \times (\vec{r}_{N_1+1}\vec{\omega}_{N_1+1}, \vec{r}_{N_1+2}\vec{\omega}_{N_1+2}, \dots, \vec{r}_{N_2}\vec{\omega}_{N_2})\dots\} \quad (1)$$

where  $\hat{A}$  is the antisymmetrizer operator, the indexes (1) and (2) represent different orthogonal wave functions (groups), and  $r_i$  and  $\omega_i$  are the electron spatial and spin coordinates, respectively.

Each group is set to be orthogonal to all others, in the same way that Generalized Valence Bond (GVB) pairs are used in the GVB-PP (Perfect Pairing) wave function. However, in a GPF groups can be treated with different methods, and more than two electrons can be put in a single group. For saturated systems, the most convenient way to divide such groups is to define one group for each electron pair involved in a chemical bond and a single group for all the electrons belonging to the core. Since core electrons play a smaller role in most chemical bonds, treating them as a single Restricted Hartree–Fock (RHF) group is a reasonable approximation. In more complex systems, such as aromatic rings,<sup>10</sup> it is necessary to define a group with more than two electrons, and carry out the calculations using a full GVB or, equivalently, a Spin-Coupled wave function.

Only a brief discussion concerning the main aspects of the method will be presented. Detailed information about the method can be found elsewhere in the literature.<sup>5</sup>

The reduced density matrices of first and second order (RDM-1 and RDM-2) for GPF wave functions are as follows:

$$\rho(\vec{r}_1, \vec{r}'_1) = \sum_{\mu=1}^{\eta} \rho^{\mu}(\vec{r}_1, \vec{r}'_1) \quad (2)$$

$$\pi(\vec{r}_1\vec{r}_2, \vec{r}'_1\vec{r}'_2) = \sum_{\mu=1}^{\eta} \pi^{\mu}(\vec{r}_1\vec{r}_2, \vec{r}'_1\vec{r}'_2) \\ + \frac{1}{2} \sum_{\mu=1}^{\eta} \sum_{\nu>\mu}^{\eta} \left[ \rho^{\mu}(\vec{r}_1, \vec{r}'_1)\rho^{\nu}(\vec{r}_2, \vec{r}'_2) - \frac{1}{2}\rho^{\mu}(\vec{r}_2, \vec{r}'_1)\rho^{\nu}(\vec{r}_1, \vec{r}'_2) \right] \quad (3)$$

where  $\eta$  is the number of groups in the GPF function. The total electronic energy expression for a GPF wave function in terms of the reduced density matrices is

$$E_{\text{GPF}} = \sum_{\mu=1}^{\eta} \left\{ \int [\hat{h}\rho^{\mu}(\vec{r}_1, \vec{r}'_1)]_{\vec{r}_1=\vec{r}_1'} d\vec{r}_1 \right. \\ \left. + \frac{1}{2} \int \left[ \frac{\pi^{\mu}(\vec{r}_1\vec{r}_2, \vec{r}'_1\vec{r}'_2)}{r_{12}} \right]_{\substack{\vec{r}_1=\vec{r}_1' \\ \vec{r}_2=\vec{r}_2'}} d\vec{r}_1 d\vec{r}_2 \right\} \\ + \frac{1}{2} \sum_{\mu=1}^{\eta} \sum_{\nu\neq\mu}^{\eta} \left\{ \frac{1}{2} \int \left[ \frac{\rho^{\mu}(\vec{r}_1, \vec{r}'_1)\rho^{\nu}(\vec{r}_2, \vec{r}'_2)}{r_{12}} \right]_{\substack{\vec{r}_1=\vec{r}_1' \\ \vec{r}_2=\vec{r}_2'}} d\vec{r}_1 d\vec{r}_2 \right\} \\ - \frac{1}{2} \sum_{\mu=1}^{\eta} \sum_{\nu\neq\mu}^{\eta} \left\{ \frac{1}{4} \int \left[ \frac{\rho^{\mu}(\vec{r}_2, \vec{r}'_1)\rho^{\nu}(\vec{r}_1, \vec{r}'_2)}{r_{12}} \right]_{\substack{\vec{r}_1=\vec{r}_1' \\ \vec{r}_2=\vec{r}_2'}} d\vec{r}_1 d\vec{r}_2 \right\} \\ + \sum_{A=1}^M \sum_{B>A}^M \frac{Z_A Z_B}{r_{AB}} \quad (4)$$

where  $\hat{h}$  is the one-electron operator, which includes both kinetic energy and electron-nuclei potential energy and  $r_{12}$  is the interelectronic distance. The expression in the first brackets stands for the intragroup energy, and the remaining part of the equation stands for the coulomb and exchange intergroup contributions, respectively. The GPF-EP method separates both  $\rho$  and  $\pi$  into interference and reference densities, the latter meaning the sum of quasi-classical densities. For instance, the interference and quasi-classical densities for a single group are

$$\rho_1^{\mu}(\vec{r}_1) = \sum_{r,s}^{N^{\mu}} {}' \langle r, s \rangle^{\mu} p(r|s) \quad (5)$$

$$\rho_{\text{QC}}^{\mu}(\vec{r}_1) = \sum_{r=1}^{N^{\mu}} (\phi_r^{\mu}(\vec{r}_1))^2 \quad (6)$$

where  $\mu$  is the selected group index,  $N^{\mu}$  is the number of electrons in this group,  $p(r|s)$  are the density matrix elements expressed in the orbital basis set, the prime character ('') on eq 5 indicates that diagonal elements ( $r = s$ ) are not included in the sum and  $\langle r,s \rangle^{\mu}$  is the interference density for orbitals  $\phi_r$  and  $\phi_s$ :

$$\langle r, s \rangle^{\mu} = \phi_r^{\mu}(\vec{r})\phi_s^{\mu}(\vec{r}) - \frac{1}{2}\xi(r,s)[(\phi_r^{\mu}(\vec{r}))^2 + (\phi_s^{\mu}(\vec{r}))^2] \quad (7)$$

where  $\xi(r,s)$  is the overlap integral between  $\phi_r^{\mu}$  and  $\phi_s^{\mu}$ . Thus, the total energy of the system can be separated as follows:

$$E[\text{tot}] = E[\text{ref}] + E[\text{I}] + E[\text{II}] + E[\text{x}] \quad (8)$$

Table 1. Some Experimental and Calculated Properties of the Studied Molecules<sup>a</sup>

	$ \Delta X_{AB} $	$(\mu_{\text{exp}}/\text{D})^b$	$(\mu_{\text{cal}}/\text{D})^c$	$(R_e/\text{\AA})^d$	$(D_e/\text{eV})^e$	$(\alpha_A/\text{au})^f$
LiH ( ${}^1\Sigma^+$ )	1.1	-5.882	-5.660	1.5954	2.516	$164.0 \pm 3.4$ (exp.)
BeH ( ${}^2\Sigma^+$ )	0.6	-0.228	-0.212	1.343	2.429	37.31
BH ( ${}^1\Sigma^+$ )	0.2	1.270	1.712	1.236	3.525	20.53
CH ( ${}^2\Pi$ )	0.4	1.460	1.459	1.124	3.649	11.26
NH ( ${}^3\Sigma^-$ )	0.9	1.539	1.649	1.045	3.893	$7.6 \pm 0.4$ (exp.)
OH ( ${}^2\Pi$ )	1.4	1.660	1.684	0.9706	4.624	5.24
HF ( ${}^1\Sigma^+$ )	1.9	-1.820	-1.825	0.9168	6.112	4.50
CO ( ${}^1\Sigma^+$ )	1.0	0.120	0.169	1.128	11.244	
LiF ( ${}^1\Sigma^+$ )	3.0	-6.325	-6.478	1.564	5.995	

<sup>a</sup>A positive dipole moment indicates A<sup>-</sup>B<sup>+</sup> polarity. <sup>b</sup>LiH: ref 30. BeH, NH: ref 31. BH: ref 32. CH: ref 33. OH: ref 34. HF: ref 35. CO: refs 28 and 29. LiF: ref 36. <sup>c</sup>This work. <sup>d</sup>Ref 37. <sup>e</sup>Calculated from the experimental values (ref 38 for LiH and ref 37 for the other molecules) of  $\omega_e$  and  $D_0$ . <sup>f</sup>Ref 39.

where  $E[\text{ref}]$  is the total reference energy,  $E[\text{I}]$  and  $E[\text{II}]$  are the first and second-order interference energies respectively, and  $E[x]$  is the total intergroup exchange energy, which arises from the antisymmetrization of the GPF wave function. It is important to emphasize that the  $E[x]$  term would not exist if the GPF wave function consisted of a single group. Consequently, the exchange term represents merely a symmetry correction to the reference energy and only arises because of the separation of the total wave function into different groups. Thus, the choice of the number of groups and the number of electrons in each group must be done with caution, since the results in terms of energy partition and its interpretation will strongly rely on the quality of this selection. In eq 8, the sum  $E[\text{ref}] + E[x]$  represents the quasi-classical contribution,  $E[\text{ref}+x]$  and  $E[\text{I}] + E[\text{II}]$  corresponds to the total interference contribution,  $E[\text{I+II}]$ .

The reference and first-order interference energies can be further separated into kinetic ( $T[\text{ref}]$  and  $T[\text{I}]$ ), electron–electron potential ( $V_{ee}[\text{ref}]$  and  $V_{ee}[\text{I}]$ ) and electron–nuclei ( $V_{en}[\text{ref}]$  and  $V_{en}[\text{I}]$ ) energies. The second-order interference energy  $E[\text{II}]$  consists exclusively of electron–electron repulsion terms and can be equivalently referred to as  $V_{ee}[\text{II}]$ . These contributions can also be divided into intragroup and intergroup contributions as follows:

$$E[\text{ref}] = \sum_{\mu=1}^{\eta} E^{\mu}[\text{ref}] + \sum_{\mu<\nu} E^{\mu,\nu}[\text{ref}] + \sum_{A=1}^M \sum_{B>A} \frac{Z_A Z_B}{r_{AB}} \quad (9)$$

$$E[\text{I}] = \sum_{\mu=1}^{\eta} E^{\mu}[\text{I}] \quad (10)$$

$$E[\text{II}] = \sum_{\mu=1}^{\eta} E^{\mu}[\text{II}] + \sum_{\mu<\nu} E^{\mu,\nu}[\text{II}] \quad (11)$$

$$E[x] = \sum_{\mu<\nu} E^{\mu,\nu}[x] \quad (12)$$

It is important to emphasize that the term “quasi-classical” is used in the present context simply to indicate that part of the energy associated with the “quasi-classical” density in the same spirit of Ruedenberg’s original work.<sup>4</sup>

### 3. COMPUTATIONAL DETAILS

The molecular systems discussed in this work comprise the first-row AH molecules (A = Li–F), CO and LiF at their respective electronic ground-states. The calculations were carried out using GPF wave functions. All the core electrons were treated as a single RHF group while the electron pair

related to the  $\sigma$ -bond between the atoms was treated with the GVB-PP method, as well as the  $\pi$  bonds for the CO molecule. The lone pairs were also treated with the GVB-PP method in all cases where they could change qualitatively (and quantitatively in a reasonable degree) the characteristics of the chemical bonds. For the OH, HF, and LiF molecules, the description of the bond is pretty much independent of how the lone pairs are treated, and therefore, these electrons were included in the RHF group. Since the interference energy is only slightly affected by the size of the basis set and the use of basis sets of moderate sizes containing polarization functions correctly describes the energy partitioning,<sup>5,6</sup> the cc-pVTZ basis set<sup>26</sup> was used in all the present calculations. A version of the VB2000<sup>27</sup> code modified by our group was used in order to perform the GPF-EP partition.

The energy partitioning was first performed for the diatomic molecules at their experimental equilibrium geometry. From this point, geometry scans were performed in order to obtain the partitioning profile from 0.60 Å to 5.00 Å, with a step size of 0.05 Å. The optimized orbitals from a given point were used as a guess for the subsequent calculation.

To get a clearer picture of the effect of interference on the electron density, interference density contour diagrams, representing the change in the electron density promoted by the interference effect were constructed. The quasi-classical electron density associated with the bond formation was also obtained. In order to do that, the quasi-classical densities of the atoms were subtracted from the quasi-classical density of the molecule. The program DensPlot, developed by our group, was used to obtain these densities.

### 4. RESULTS AND DISCUSSION

Before going into details of our calculations, it would be instructive to briefly review some of the qualitative and semiquantitative criteria used to predict the polarity of a bond. The simplest and widely used criterion is based on the difference of electronegativity ( $\Delta X_{AB}$ ) of the two atoms making the bond. According to this criterion the larger the  $\Delta X_{AB}$  the larger is the polarity of the bond and its dipole moment, and for  $\Delta X_{AB} \approx 2$  or larger the bond is considered “ionic”. Although quite simple to use, this criterion can be very deceiving as illustrated by the experimental results for the set of molecules considered.

Table 1 shows some experimental data for the ground electronic state of the studied molecules and the respective difference of electronegativity (Pauling scale). For the AH molecules, according to the  $\Delta X_{AB}$  criterion, the HF molecule should be the most polar and BH the less polar bond, in

disagreement with the experimental dipole moments. In addition, the bond in HF and LiF should be considered “ionic” ( $\text{H}^+\text{F}^-$  and  $\text{Li}^+\text{F}^-$ ), a point to be further discussed in the paper. Moreover, this criterion furnishes wrong predictions not only of relative magnitudes of dipole moments but also of their signs. For example, according to this criterion one would wrongly predict that CO ( $\Delta X_{\text{CO}} = 1.0$ ;  $\mu = 0.120 \text{ D}$ ) exhibits a larger dipole moment than CH ( $\Delta X_{\text{CH}} = 0.4$ ;  $\mu = 1.460 \text{ D}$ ) and because  $X_{\text{O}} > X_{\text{C}}$ , that the negative end of the dipole moment should be on the oxygen atom ( $\text{C}^+\text{O}^-$ ) contrary to the experimental observations.<sup>28,29</sup>

Another commonly used procedure to establish the polarity of a bond and its “ionic” character is to consider the formation of an ion-pair from the respective neutral atoms and compare the energy of the pair at infinite separation and at the experimental internuclear distance. For purely ionic bonds, the resulting energy should be comparable to the dissociation energy at the equilibrium distance ( $D_e$ ). For LiH and HF, assuming the polarity suggested by the respective  $\Delta X$ s, one can write, at the respective internuclear distances ( $R_e$ ):

$$\begin{aligned} E_{\text{ionic}}(\infty) - E_{\text{atomic}}(E_{\text{Li}} + E_{\text{H}}) \\ = \text{IP(Li)} - \text{EA(H)} - \frac{14.40}{R_e(\text{\AA})} + E_{\text{rep}} \end{aligned} \quad (14.1)$$

$$\begin{aligned} E_{\text{ionic}}(\infty) - E_{\text{atomic}}(E_{\text{F}} + E_{\text{H}}) \\ = \text{IP(H)} - \text{EA(F)} - \frac{14.40}{R_e(\text{\AA})} + E_{\text{rep}} \end{aligned} \quad (14.2)$$

where IP is the ionization potential, EA is the electron affinity, the third term represents the Coulombic attraction between the ions (in eV), and the last term takes into account the repulsion among the internal electrons of the atoms (overlap repulsion) as they approach each other. This last term can be neglected in a preliminary analysis since the internal orbitals of Li and F are much more compact than the 1s orbital of the hydrogen atom but one must keep in mind that this term will be certainly larger for the HF molecule which has a much shorter bond distance.

Using the experimental data in eqs 14.1 and 14.2 one obtains  $D_e$  (LiH) = 4.41 eV, almost twice the experimental value, and  $D_e$  (HF) = 5.56 eV, just 0.56 eV below the experimental value. Therefore, according to these results HF should exhibit a much stronger ionic character than LiH and consequently a larger dipole moment, exactly in opposition to the experimental data. It is true that the consideration of the term  $E_{\text{rep}}$  could improve a bit the result for LiH but not enough to bring it down to the experimental value (2.51 eV).

It is clear, from the discussion above, that the correct description of polar bonds requires more accurate models than the ones based on difference of electronegativity or simple electrostatic. More quantitative schemes have been proposed and can be found in the literature.<sup>11–15</sup>

#### 4.1. Interference Energies for the Studied Molecules.

Table 2 shows the total interference energy ( $E[\text{I+II}]$ ) partitioning of the  $\sigma$ -bonds for the studied molecules into kinetic ( $T[\text{I}]$ ) and potential ( $V[\text{I+II}]$ ) contributions. For the CO molecule the contributions of the  $\sigma$  and  $\pi$  bonds to  $T[\text{I}]$  and  $V[\text{I+II}]$  are also shown. It is possible to see, in all cases, that the stabilization promoted by the interference term comes from the kinetic contribution. This result is in agreement with previous works<sup>1–10</sup> and represents another evidence for the role of the kinetic energy to chemical binding. Moreover, as the

**Table 2. Kinetic ( $T[\text{I}]$ ), Potential ( $V[\text{I+II}]$ ), and Total ( $E[\text{I+II}]$ ) Interference Contributions for the Bonds of the Studied Molecules<sup>a</sup>**

molecule	$T[\text{I}]$	$V[\text{I+II}]$	$E[\text{I+II}]$
LiH	-66.5	14.7	-51.8
BeH	-94.7	27.9	-66.8
BH	-121.7	46.0	-75.7
CH	-154.3	64.8	-89.5
NH	-183.4	83.6	-99.8
OH	-203.5	103.1	-100.3
HF	-219.7	110.4	-109.3
CO $\sigma$	-271.9	147.7	-124.3
$\pi$	-144.9	70.2	-74.7
LiF	-118.4	30.1	-88.3

<sup>a</sup>Energies are in kcal mol<sup>-1</sup>.

equilibrium bond distance decreases along the first-row AH series, the interference energy becomes more negative. Figure 1 shows the correlation between these two properties for the AH molecules.

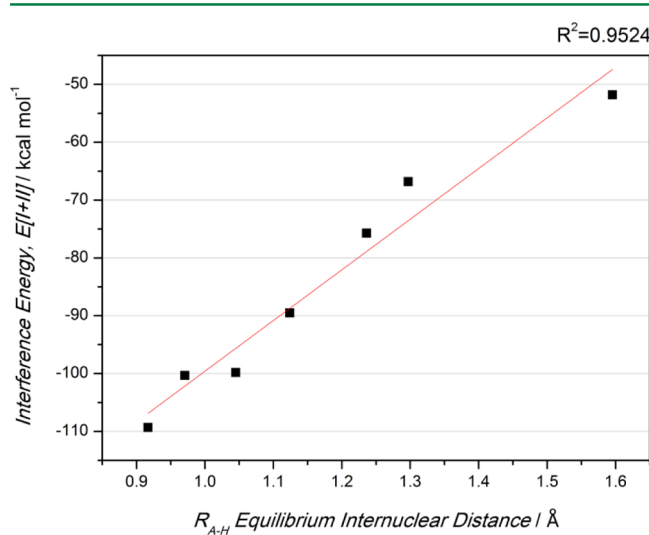


**Figure 1.** Correlation between the equilibrium internuclear distance and the interference energy for the  $\sigma$ -bond of the first-row AH molecules.

Figure 2 shows the energy partitioning of the studied molecules into interference and quasi-classical contributions along the respective Potential Energy Surfaces (PES). Although the optimal bond lengths are defined by a combination of both effects, the main contribution to the depth of the potential well (in most cases the sole contribution) comes from the interference term. This is a strong evidence that despite the difference of electronegativity between the atoms involved, all of the molecules described herein form typical covalent bonds, in agreement to the findings of Layton and Ruedenberg for LiH, BH, NH, and HF.<sup>40</sup> This result also strongly suggests that the same phenomenon seems to be responsible for the formation of polar and nonpolar bonds: the interference effect between one-electron eigenstates. Therefore, the interference effect could pave the way to the unification of the chemical bonding concept. The validity of this hypothesis, of course, must be verified by similar calculations for many other classes of polar compounds for which calculations are now in progress.

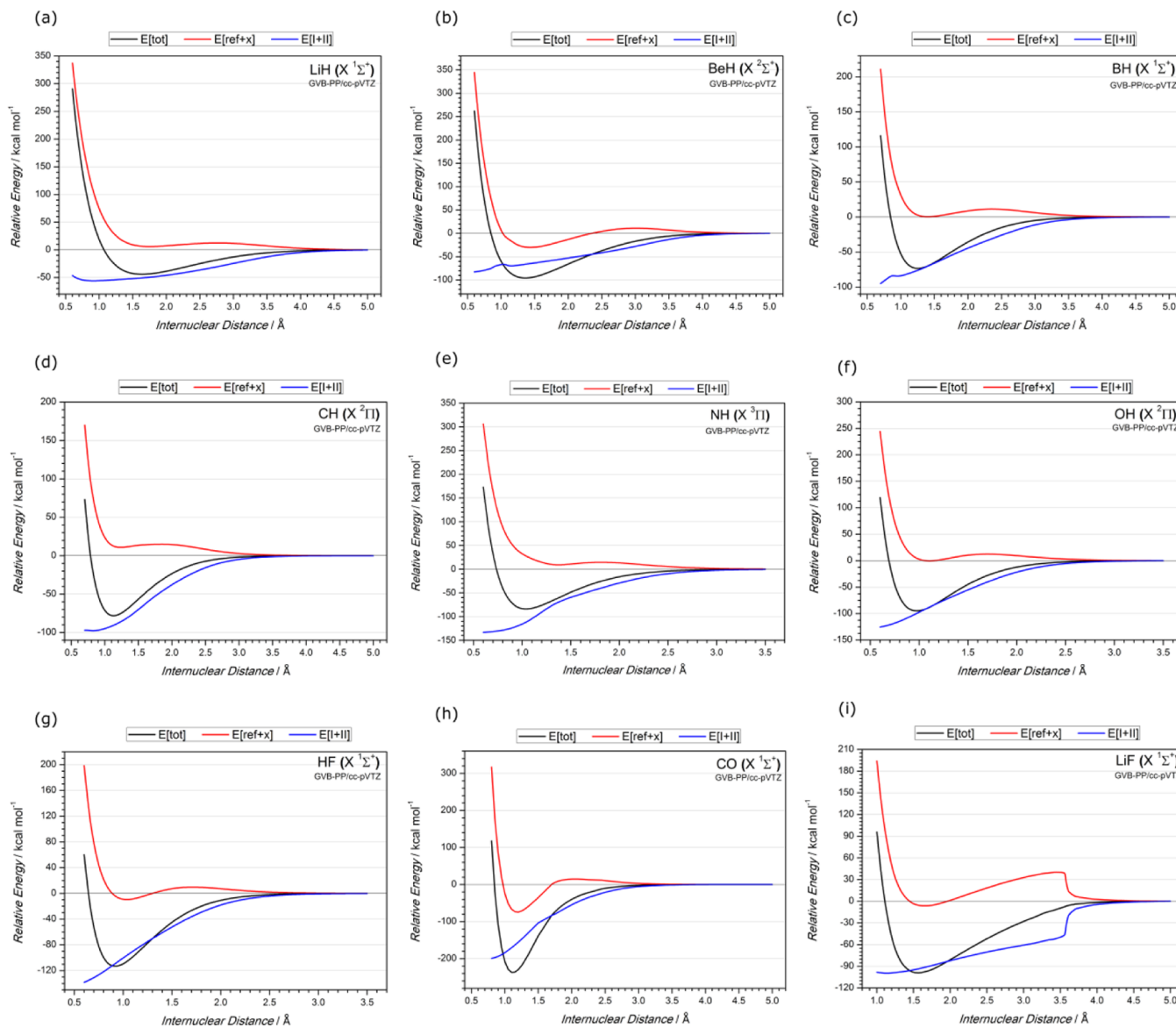


**Figure 2.** Energy partitioning along the PES of the studied molecules: (a) LiH, (b) BeH, (c) BH, (d) CH, (e) NH, (f) OH, (g) HF, (h) CO, (i) LiF.

#### 4.2. Interference Densities for the Studied Molecules.

The analysis of the effect of quantum interference on the electron density can reveal aspects of the bonding mechanism for polar molecules. Figure 3 shows the interference density, the quasi-classical density (as described in section 3) and the sum of both densities for LiH, HF, and LiF molecules. As expected, the quasi-classical density associated with the formation of the molecule displaces electron density to regions (in red) next to the more electronegative atom (Figure 3a.1, b.1, c.1). However, this effect does not contribute to the bond formation, as shown in Figure 2. On the other hand, the interference effect moves part of the electron density from the more electronegative atom back to the bonding region (in red), as shown in Figure 3a.2, b.2, and c.2. Although relatively smaller than the quasi-classical density, the interference density attenuates the increase of electron density at the electronegative site and accounts for the majority of the stabilization of the molecular system. Therefore, it is the transfer of electron density from the more electronegative atom to the bonding region promoted by the quantum interference effect that causes the formation of a polar molecule.

The CO molecule is particularly interesting because the quasi-classical density associated with the  $\sigma$  bond (Figure 4a.1) shows electronic charge being displaced from the oxygen atom to the less electronegative carbon atom, in a clear indication of the propensity to form a dative ( $C \leftarrow O$ )  $\sigma$  bond, although this charge displacement is not the dominant effect for the formation of the bond, as shown in Figure 2h. On the other hand, the interference effect (Figure 4a.2) displaces charge from both atoms to the bond region and responds for the formation of the  $\sigma$  bond (Figure 4a.3). In the  $\pi$  space, the quasi-classical and interference densities counteract displacing electronic density from the carbon to the oxygen atom (Figures 4b.1, b.2, and b.3).

Figure 5 shows the interference density for the other studied molecules where it is possible to see that the electron density displacement from the nuclei regions to the bonding region increases as the molecule equilibrium bond length decreases. From Figure 4, it is also evident that the displacement of electron density from the atomic regions to the bond region due to interference depends on the difference of electronegativity, being larger for the more electronegative atom.

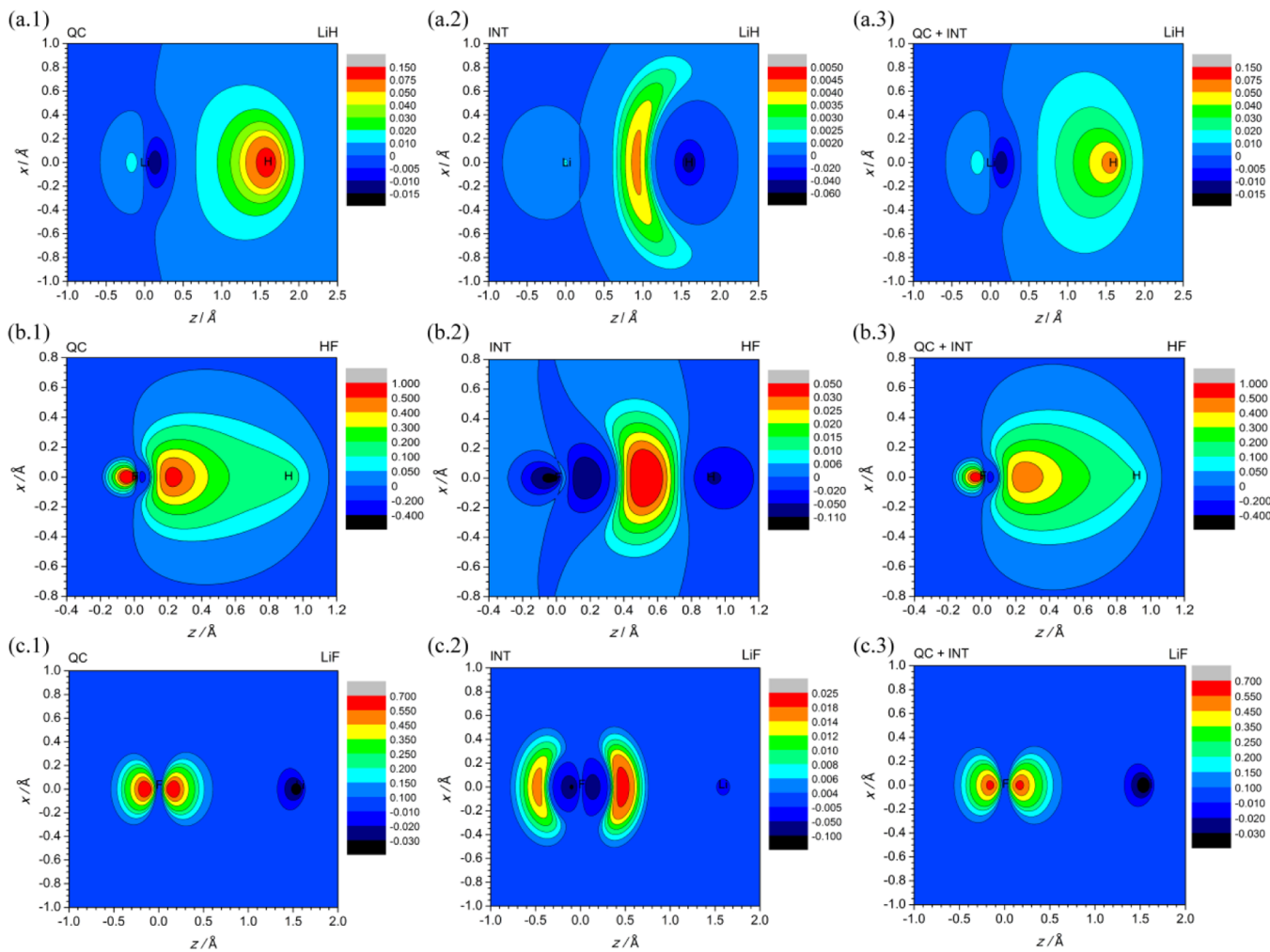


**Figure 3.** Quasi-classical (QC), interference (INT), and total (QC + INT) density plots for (a) LiH, (b) HF, and (c) LiF.

From the results presented in section 4, a simple mechanistic picture of bond formation for polar molecules can be envisaged:

- with the atoms far from each other, there is no overlap between the orbitals involved in the bond and, thus, they do not interfere. At any distance larger than the bond dissociation limit, the quasi-classical density is given by the sum of the squares of these orbitals;
- as the atoms approach, electrostatic effects change the quasi-classical density in such a way that electron density is displaced from the less electronegative to the more electronegative atom;
- however, orbitals are now allowed to interfere, changing the total density from a sum of squares to the square of the sum of the two orbitals;
- the resulting interference term between the two orbitals modifies the shape of the density, displacing electron density from regions next to the nuclei (mainly from the more electronegative atom) to the bonding region. This effect stabilizes the system and a covalent polar chemical bond is formed.

#### 4.3. Dipole Moments of LiH, HF, LiF and CO Molecules.

Having established that none of the bonds are ionic, it remains to explain why these four molecules present dipole moments which are quite different from what would be expected from the

simple and widely used models discussed at the beginning of this section.

The large dipole moment of LiH is related to its very large polarizability (Table 1) compared to that of the hydrogen atom (4.5a.u.), and not to the formation of an “ionic” bond. Thus, as the Li atom approaches the H atom, the electric field at the Li atom due to the H nuclear charge promotes a very large distortion of the Li electronic density toward the H atom. To show that this is really the case, we solved self-consistently for the Li atom in the presence of a unit point charge (+) located at exactly the position of the H atom in the LiH molecule at its equilibrium distance. Figure 6 shows four different contours of the Li bonding orbital in the molecule compared to the Li atomic orbital in the presence of the point charge. It is clear from this comparison that the large distortion of the Li electron density is due to a quasi-classical effect (polarization) and not a covalent one and that the large dipole moment of the molecule has nothing to do with the formation of an “ionic” bond. Another point to be noticed is that the dipole moment is not as large as predicted from an “ionic” bond because quantum interference acts against polarization, displacing density from the H atom region to the bond region as discussed before. Therefore, quantum interference not only responds for the formation of the covalent bond but also for the correct value of the dipole moment.

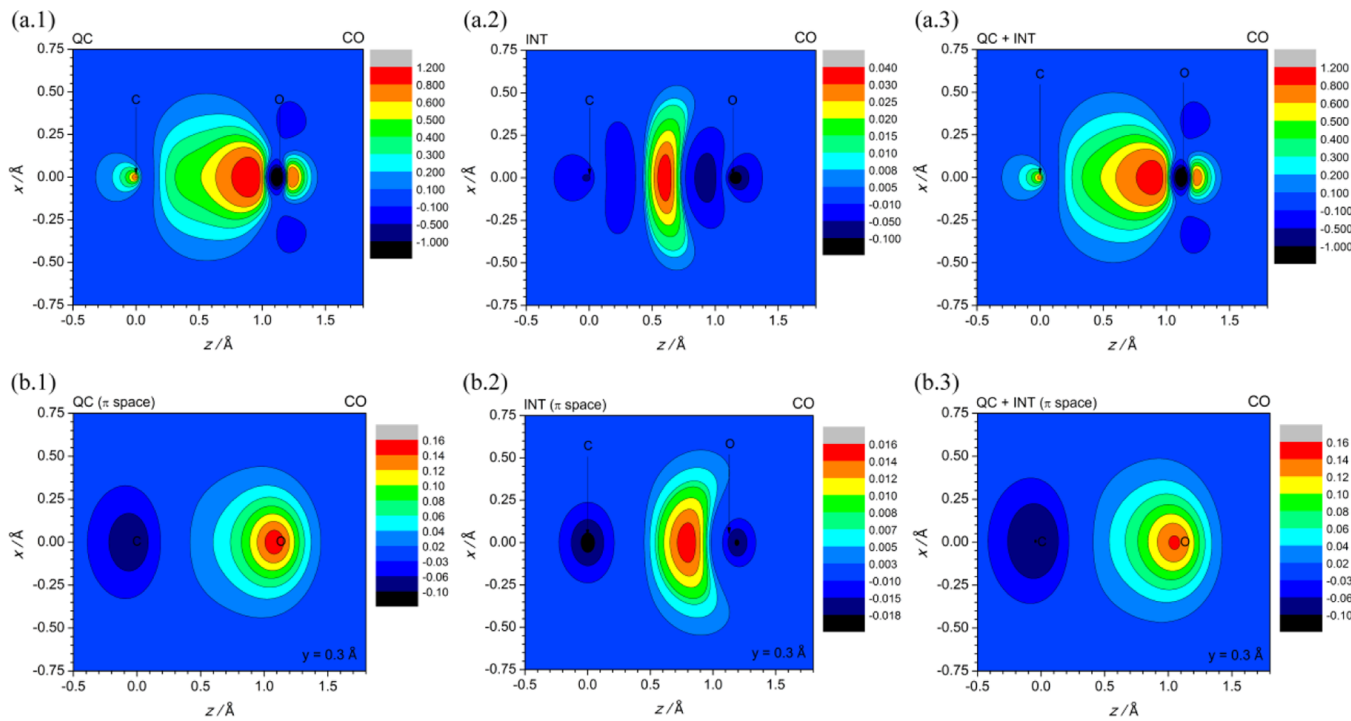


**Figure 4.** Quasi-classical (QC), interference (INT) and total (QC + INT) density plots for CO: (a)  $\sigma$  bond, (b)  $\pi$  bond.

The LiH molecule has been extensively investigated, from both theoretical and experimental points of view,<sup>30,41–56</sup> and it is quite interesting to point out that this molecule is almost universally used as the simplest example of an “ionic” bond in the same way that the potential energy surfaces of its “ionic” and covalent states are used to exemplify the noncrossing rule. However, most of the MO-type studies concentrated efforts in calculating multipole moments and spectroscopic constants, at various levels of theory, without paying much attention to the nature of the chemical bond. Therefore, one might think that the attribution of ionic character to the LiH molecule should be somehow related to classical VB calculations where ionic structures must be included to promote polarization because the atomic orbitals are kept fixed as the atoms approach each other. However, even the earliest classical VB calculations,<sup>48</sup> as well as more recent ones,<sup>49</sup> indicate that the bond in LiH is covalent as long as the tableau corresponding to the  $1s(\text{Li})^2 2p_z(\text{Li})^1 1s(\text{H})^1$  is included in the VB expansion to allow for  $sp_{\text{Li}}$  hybridization. Moreover, when this configuration is included in ab initio VB calculations<sup>56</sup> to promote polarization, not only VB predicts a covalent bond but the correct dipole moment as well.

In the other extreme of the periodic table, we have the HF molecule, also extensively studied.<sup>35,40,57–65</sup> According to the simple criteria discussed before, HF should present the largest dipole moment among the AH molecules and a pure “ionic” bond, in total disagreement to the experimental results. Theoretical calculations of the HF dipole moment, using either the VB or MO model, are, in general, in good agreement with experiments.<sup>57,58,60–65</sup> On the other hand, there is no agreement regarding the nature of the chemical bond.<sup>12,63,64</sup>

The same reasoning used for the LiH molecule can be applied to HF. For this molecule, the situation is quite different because the atomic polarizabilities are of the same order of magnitude ( $\alpha_{\text{H}} = 4.5$  au and  $\alpha_{\text{F}} = 3.7$  au) and, therefore, one should expect that the bonding orbitals ( $1s_{\text{H}}$  and  $2p_{z\text{F}}$ ) would

be almost equally polarized toward the other atom. This is exactly what happens as shown in Figure 7. The quasi-classical effect (polarization) displaces the atomic densities to the bond region and the quantum interference changes slightly this distribution resulting in a covalent bond and a much smaller dipole moment than LiH.

The fact that the LiF molecule presents the largest dipole moment among the studied molecules and also the largest  $\Delta X_{\text{AB}}$  may give the false impression that at least for this molecule a simple qualitative model can correctly predict the polarity of the bond. The prediction may be correct but for the wrong reason. Here, again, is the difference of polarizabilities ( $\alpha_{\text{Li}} = 164$  au and  $\alpha_{\text{F}} = 3.7$  au) that responds for the large dipole moment of the molecule. Similarly to the LiH case, we solved self-consistently for the Li atom in the presence of a +4 point charge (which is approximately the effective nuclear charge experienced by an electron in the  $2p$  orbital of the fluorine atom) located at exactly the position of the F atom in the LiF molecule at its equilibrium distance. Figure 8 shows superimposed contour diagrams for the Li atomic valence orbital in the presence of the point charge and the Li bonding orbital in the LiF molecule, respectively.

As in the case of LiH, the valence orbital of the Li atom is strongly polarized in the direction of the point charge and also in the presence of the fluorine atom, although the shapes are not as similar as in the case of LiH. This difference in shape has to do with the fact that, contrary to the LiH case, in the LiF molecule the induced field is not as spherically symmetric, favoring a more effective mixing of the  $2s$  and  $2p$  orbitals of Li along the molecular axis.

The dipole moment of CO represents a pathological problem for the MO model. A large number of calculations has been reported<sup>66–69</sup> and in spite of the size of the basis sets used, the dipole moment of CO at the Hartree–Fock level is wrong by 100% in magnitude and has the wrong sign. The most systematic study was done by Scuseria et al.<sup>66</sup> who used

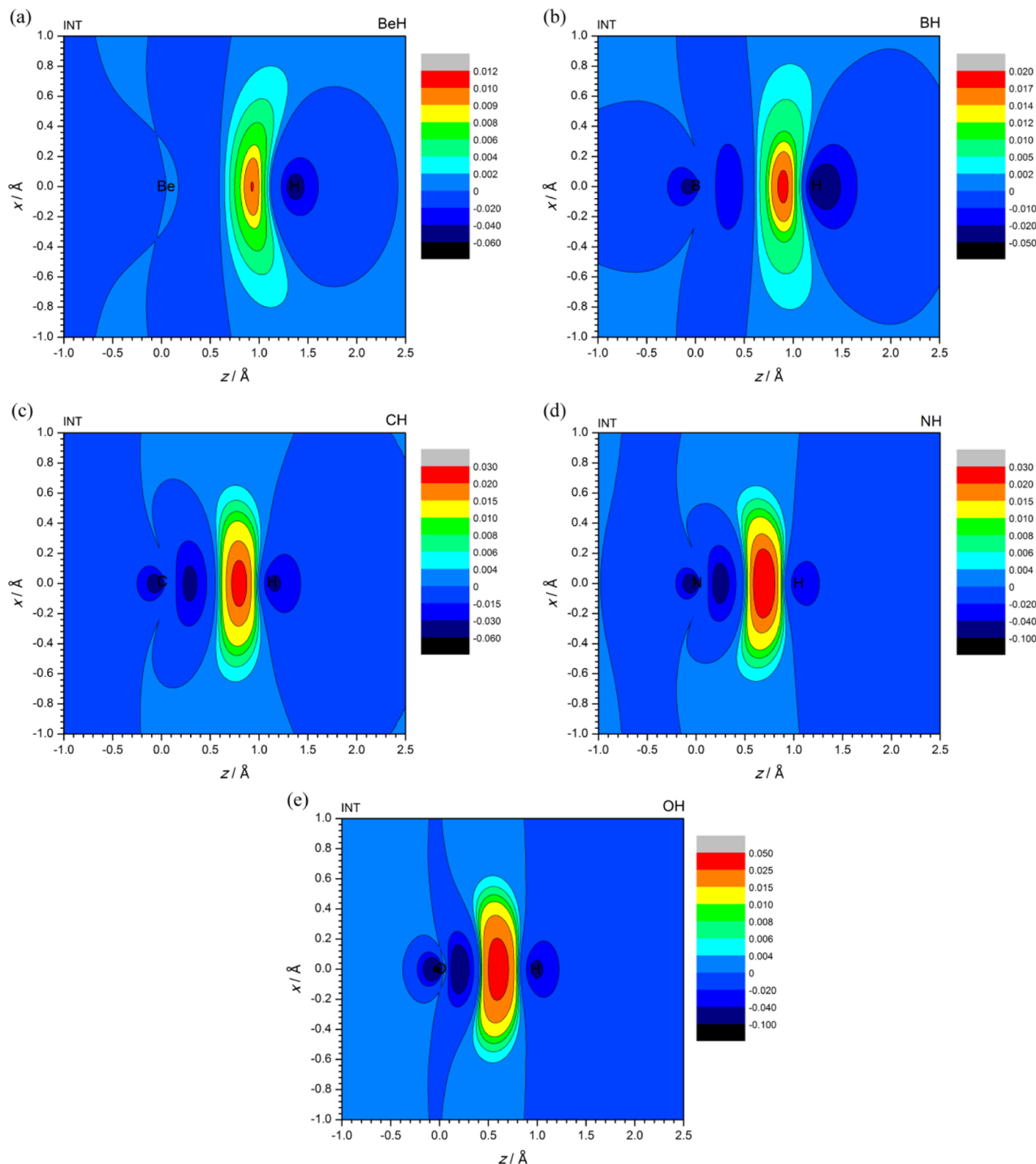


**Figure 5.** Interference density contour diagrams for (a) BeH, (b) BH, (c) CH, (d) NH, and (e) OH.

basis sets as large as 10s9p4d2f1g but still obtained a dipole moment of 0.2653 D ( $\mu_{\text{exp}} = -0.120$  D) and the wrong sign. The numerical Hartree–Fock result of Laaksonen et al.<sup>67</sup> ( $\mu = 0.2650$  D) is a clear indication that the problem is not the quality and size of the basis sets but the inability of the MO model to correctly describe the electronic density of the molecule. As usual, any failures of the HF-MO models are attributed to correlation effects and, in the particular case of the dipole moment of CO, mainly to the lack of correlation in the  $\pi$  space. Correlation effects were systematically introduced by Scuseria et al.<sup>66</sup> and Barnes et al.<sup>68</sup> at several levels of Many Body Perturbation Theory (MBPT) and Coupled Cluster

(CC). The best values of the dipole moment were obtained at the CCSD(T) level of calculation [ $(\mu = 0.125$  D)<sup>66</sup> and  $(\mu = 0.110$  D)<sup>68</sup>] in very good agreement with the experimental value.

On the other hand, the fact that an independent particle model, such as GVB, is able to correctly predict the magnitude and the sign of the dipole moment of CO is an evidence that the correlation treatment is somehow compensating the inability of the MO model to describe the  $\sigma$  dative bond responsible for the displacement of charge from the oxygen atom to the carbon atom along the molecular axis, as shown in the GVB diagram of Figure 9.

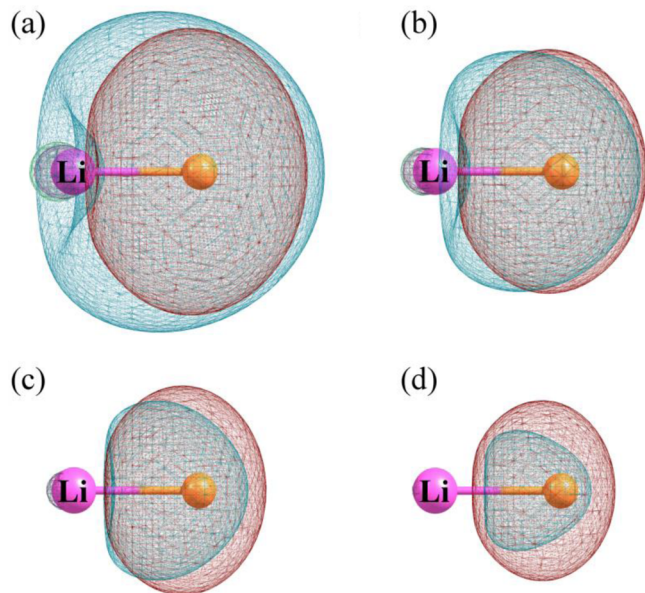


**Figure 6.** Contour diagrams of the Li bonding orbital in LiH (blue) and the Li atomic valence orbital in the presence of a positive +1 point charge (red). Contour values: (a) 0.04; (b) 0.06; (c) 0.08; (d) 0.10.

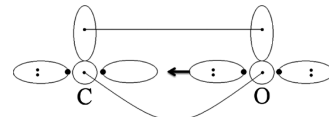


**Figure 9.** GVB diagram for the ground-state of CO.

## 5. CONCLUSIONS

The Generalized Product Function Energy Partitioning (GPF-EP) method has been applied to a set of molecules, AH (A = Li, Be, B, C, N, O, F), CO and LiF, with quite different dipole moments, in order to investigate the role played by the quantum interference effect in the formation of polar chemical bonds. The calculations were carried out with GPF wave functions treating all the core electrons as a single Hartree–Fock group and the bonding electrons at the Generalized Valence Bond Perfect-Pairing (GVB-PP) level.

The results of the energy partitioning into interference and quasi-classical contributions along the respective Potential Energy Surfaces (PES) show that the main contribution to the depth of the potential wells comes from the interference term, which is an indication that all the AH molecules form typical covalent bonds. In all cases, the stabilization promoted by the interference term comes from the kinetic contribution, in agreement with previous studies. These results strongly suggest that the same phenomenon seems to be responsible for the formation of polar and nonpolar bonds: the interference effect between one-electron eigenstates.

The analysis of the effect of quantum interference on the electron density reveals that while polarization effects (quasi-classical) tend to displace electronic density from the most polarizable atom toward the less polarizable one, interference (quantum effects) counteracts by displacing electronic density to the bond region, giving rise to the right electronic density and dipole moment.

Based on this analysis a simple mechanistic picture of bond formation for polar molecules can be depicted: (a) at any distance larger than the bond dissociation limit, as the bonding orbitals do not overlap the total density is given by the quasi-classical density: the sum of the squares of the orbitals; (b) electron density is displaced from the less electronegative to the more electronegative atom by electrostatic effects as the atoms approach; (c) since orbitals are now allowed to interfere, the total density changes from a sum of squares to the square of the sum of the two orbitals; (d) interference modifies the shape of the density, displacing electron density from regions next to the nuclei (mainly from the more electronegative atom) to the bonding region. This effect stabilizes the system and the formation of a covalent polar chemical bond is accomplished.

## ■ AUTHOR INFORMATION

### Corresponding Author

\*Tel.: +55-21-3938 ext. 7563. Fax: +55-21-3938 ext. 7265.  
Email: chaer01@gmail.com.

### Notes

The authors declare no competing financial interest.

## ■ ACKNOWLEDGMENTS

We acknowledge FAPERJ, CAPES, and CNPq for financial support.

## ■ REFERENCES

- (1) Nascimento, M. A. C. The Nature of the Chemical Bond. *J. Braz. Chem. Soc.* 2008, 19.

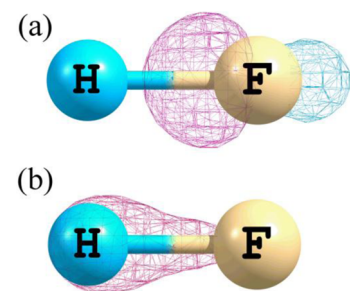


**Figure 7.** (a) Fluorine 2p<sub>z</sub> orbital and (b) hydrogen 1s orbital. Contour value: 0.40.

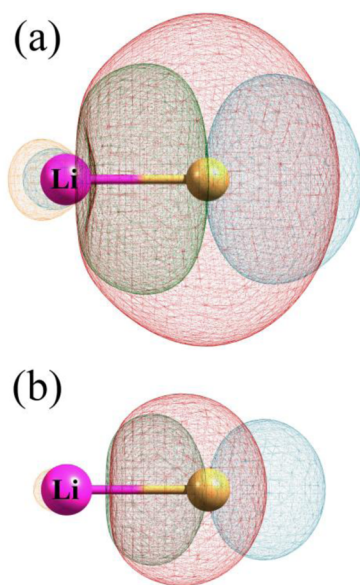


**Figure 8.** Contour diagrams of the Li bonding orbital in LiF (blue and green) and the Li atomic valence orbital in the presence of a positive +4 point charge (red). Contour values: (a) 0.04; (b) 0.10.

- (2) Wilson, C. W., Jr.; Goddard, W. A. Exchange Kinetic Energy, Congradience, and Chemical Binding. *Chem. Phys. Lett.* **1970**, *5*, 45–49.
- (3) Kutzelnigg, W. The Physical Origin of the Chemical Bond. In *Theoretical Models of Chemical Bonding: Part 2*; Maksic, Z. B., Ed.; Springer-Verlag: Berlin, 1990; pp 1–43.
- (4) Ruedenberg, K. The Physical Nature of the Chemical Bond. *Rev. Mod. Phys.* **1962**, *34*, 326–376.
- (5) Cardozo, T. M.; Nascimento, M. A. C. Energy Partitioning for Generalized Product Functions: The Interference Contribution to the Energy of Generalized Valence Bond and Spin Coupled Wave Functions. *J. Chem. Phys.* **2009**, *130*, 104102.
- (6) Cardozo, T. M.; Nascimento, M. A. C. Chemical Bonding in the N(2) Molecule and the Role of the Quantum Mechanical Interference Effect. *J. Phys. Chem. A* **2009**, *113*, 12541–12548.
- (7) Cardozo, T. M.; Nascimento Freitas, G.; Nascimento, M. A. C. Interference Effect and the Nature of the  $\pi$ -Bonding in 1,3-Butadiene. *J. Phys. Chem. A* **2010**, *114*, 8798–8805.
- (8) Fantuzzi, F.; Cardozo, T. M.; Nascimento, M. A. C. The Role of Quantum-Mechanical Interference and Quasi-classical Effects in Conjugated Hydrocarbons. *Phys. Chem. Chem. Phys.* **2012**, *14*, 5479–5488.
- (9) Vieira, F. S.; Fantuzzi, F.; Cardozo, T. M.; Nascimento, M. A. C. Interference Energy in C–H and C–C Bonds of Saturated Hydrocarbons: Dependence on the Type of Chain and Relationship to Bond Dissociation Energy. *J. Phys. Chem. A* **2013**, *117*, 4025–4034.
- (10) Cardozo, T. M.; Fantuzzi, F.; Nascimento, M. A. C. The Noncovalent Nature of the Molecular Structure of the Benzene Molecule. *Phys. Chem. Chem. Phys.* **2014**, DOI: 10.1039/c3cp55256j.
- (11) Bader, R. F. W.; Henneker, W. H. The Ionic Bond. *J. Am. Chem. Soc.* **1965**, *87*, 3063–3068.
- (12) Sini, G.; Maitre, P.; Hiberty, P. C.; Shaik, S. S. Covalent, Ionic and Resonating Single Bonds. *J. Mol. Struct. THEOCHEM* **1991**, *229*, 163–188.
- (13) Chesnut, D. B. A Simple Definition of Ionic Bond Order. *J. Chem. Theory Comput.* **2008**, *4*, 1637–1642.
- (14) Shaik, S.; Danovich, D.; Wu, W.; Hiberty, P. C. Charge-Shift Bonding and Its Manifestations in Chemistry. *Nat. Chem.* **2009**, *1*, 443–449.
- (15) Gámez, J. A.; Yañez, M. [FAAF]: (A = O, S, Se, Te) or How Electrostatic Interactions Influence the Nature of the Chemical Bond. *J. Chem. Theory Comput.* **2013**, *9*, 5211–5215.
- (16) Goddard, W. A.; Harding, L. B. The Description of Chemical Bonding From AB Initio Calculations. *Annu. Rev. Phys. Chem.* **1978**, *29*, 363–396.
- (17) Kovács, A.; Esterhuyse, C.; Frenking, G. The Nature of the Chemical Bond Revisited: An Energy-Partitioning Analysis of Nonpolar Bonds. *Chemistry* **2005**, *11*, 1813–1825.
- (18) Ponec, R.; Cooper, D. L. Anatomy of Bond Formation. Bond Length Dependence of the Extent of Electron Sharing in Chemical Bonds from the Analysis of Domain-Averaged Fermi Holes. *Faraday Discuss.* **2007**, *135*, 31.
- (19) Ponec, R.; Cooper, D. L. Anatomy of Bond Formation. Domain-Averaged Fermi Holes as a Tool for the Study of the Nature of the Chemical Bonding in Li(2), Li(4), and F(2). *J. Phys. Chem. A* **2007**, *111*, 11294–11301.
- (20) Bitter, T.; Ruedenberg, K.; Schwarz, W. H. E. Toward a Physical Understanding of Electron-Sharing Two-Center Bonds. I. General Aspects. *J. Comput. Chem.* **2007**, *28*, 411–422.
- (21) Harrison, J. A. The Hyperbolic Chemical Bond: Fourier Analysis of Ground and First Excited State Potential Energy Curves of HX (X = H–Ne). *J. Phys. Chem. A* **2008**, *112*, 8070–8085.
- (22) Ruedenberg, K.; Schmidt, M. W. Physical Understanding through Variational Reasoning: Electron Sharing and Covalent Bonding. *J. Phys. Chem. A* **2009**, *113*, 1954–1968.
- (23) Ando, K. Electron Wave Packet Modeling of Chemical Bonding: Floating and Breathing Minimal Packets with Perfect-Pairing Valence-Bond Spin Coupling. *Chem. Phys. Lett.* **2012**, *523*, 134–138.
- (24) Jacobsen, H. Bond Descriptors Based on Kinetic Energy Densities Reveal Regions of Slow Electrons—Another Look at Aromaticity. *Chem. Phys. Lett.* **2013**, *582*, 144–147.
- (25) Mayer, I. Covalent Bonding: The Role of Exchange Effects. *J. Phys. Chem. A* **2014**, *118*, 2543–2546.
- (26) Dunning, T. H. Gaussian Basis Sets for Use in Correlated Molecular Calculations. I. The Atoms Boron through Neon and Hydrogen. *J. Chem. Phys.* **1989**, *90*, 1007.
- (27) Li, J.; McWeeny, R. VB2000: Pushing Valence Bond Theory to New Limits. *Int. J. Quantum Chem.* **2002**, *89*, 208–216.
- (28) Rosenblum, B.; Nethercot, A.; Townes, C. Isotopic Mass Ratios, Magnetic Moments, and the Sign of the Electric Dipole Moment in Carbon Monoxide. *Phys. Rev.* **1958**, *109*, 400–412.
- (29) Muenter, J. S. Electric Dipole Moment of Carbon Monoxide. *J. Mol. Spectrosc.* **1975**, *55*, 490–491.
- (30) Wharton, L.; Gold, L. P.; Klemperer, W. Dipole Moment of Lithium Hydride. *J. Chem. Phys.* **1960**, *33*, 1255.
- (31) Johnson III, R. D. NIST Computational Chemistry Comparison and Benchmark Database. <http://cccbdb.nist.gov/> (accessed February 8, 2014).
- (32) Thomson, R.; Dalby, F. W. An Experimental Determination of the Dipole Moments of the X( $^1\Sigma$ ) and A( $^1\Pi$ ) States of the BH Molecule. *Can. J. Phys.* **1969**, *47*, 1155–1158.
- (33) Phelps, D.; Dalby, F. Experimental Determination of the Electric Dipole Moment of the Ground Electronic State of CH. *Phys. Rev. Lett.* **1966**, *16*, 3–4.
- (34) Powell, F. X.; Lide, D. R. Improved Measurement of the Electric-Dipole Moment of the Hydroxyl Radical. *J. Chem. Phys.* **1965**, *42*, 4201.
- (35) Weiss, R. Stark Effect and Hyperfine Structure of Hydrogen Fluoride. *Phys. Rev.* **1963**, *131*, 659–665.
- (36) Trischka, J. W. On the Internuclear Distance and Dipole Moment of the LiF Molecule. *J. Chem. Phys.* **1952**, *20*, 1811.
- (37) Huber, K.; Herzberg, G. *Molecular Spectra and Molecular Structure. IV. Constants of Diatomic Molecules*; 1st ed.; Van Nostrand, 1979.
- (38) Tung, W.-C.; Pavanello, M.; Adamowicz, L. Very Accurate Potential Energy Curve of the LiH Molecule. *J. Chem. Phys.* **2011**, *134*, 064117.
- (39) Schwerdtfeger, P. Table of Experimental and Calculated Static Dipole Polarizabilities for the Electronic Ground States of the Neutral Elements (In Atomic Units). <http://ctcp.massey.ac.nz/Tablepol2014.pdf> (accessed Feb. 8, 2014).
- (40) Layton, E. M.; Ruedenberg, K. Chemical Binding in Diatomic Hydride Molecules. *J. Phys. Chem.* **1964**, *68*, 1654–1676.
- (41) Karo, A. M.; Olson, A. R. Configuration Interaction in the Lithium Hydride Molecule. I. A Determinantal AO Approach. *J. Chem. Phys.* **1959**, *30*, 1232.
- (42) Kahalas, S. L.; Nesbet, R. K. Electronic Structure of LiH and Quadrupole Moment of Li $^7$ . *J. Chem. Phys.* **1963**, *39*, 529.
- (43) Boys, S. F.; Handy, N. C. A First Solution, for LiH, of a Molecular Transcorrelated Wave Equation by Means of Restricted Numerical Integration. *Proc. R. Soc. A Math. Phys. Eng. Sci.* **1969**, *311*, 309–329.
- (44) Palke, W. E.; Goddard, W. A., III Electronic Structure of LiH According to a Generalization of the Valence-Bond Method. *J. Chem. Phys.* **1969**, *50*, 4524.
- (45) Partridge, H.; Langhoff, S. R. Theoretical Treatment of the X  $^1\Sigma^+$ , A  $^1\Sigma^+$ , and B  $^1\Pi$  States of LiH. *J. Chem. Phys.* **1981**, *74*, 2361.
- (46) Partridge, H.; Langhoff, S. R.; Stwalley, W. C.; Zemke, W. T. Theoretical Study of the Dipole Moment Function of the A  $1\Sigma^+$  State of LiH. *J. Chem. Phys.* **1981**, *75*, 2299.
- (47) Roos, B. O.; Sadlej, A. J. Polarized Basis Sets for Accurate Predictions of Molecular Electric Properties. Electric Moments of the LiH Molecule. *Chem. Phys.* **1985**, *94*, 43–53.
- (48) Miller, J.; Friedman, R. H.; Hurst, R. P.; Matsen, F. A. Electronic Energy of LiH and BeH. *J. Chem. Phys.* **1957**, *27*, 1385.

- (49) Mo, Y.; Wu, W.; Zhang, Q. Valence Bond Description for the Ground State and Several Low-Lying Excited States of LiH. *J. Mol. Struct. THEOCHEM* **1993**, *283*, 237–249.
- (50) Yamada, C.; Hirota, E. Infrared Diode Laser Spectroscopy of Lithium Hydride. *J. Chem. Phys.* **1988**, *88*, 6702.
- (51) Politzer, P. Electronic Density Distribution in Lithium Hydride. *J. Chem. Phys.* **1966**, *45*, 451.
- (52) Bader, R. F. W. Molecular Charge Distributions and Chemical Binding. II. First-Row Diatomic Hydrides, AH. *J. Chem. Phys.* **1967**, *47*, 3381.
- (53) Hirshfeld, F. L.; Rzotkiewicz, S. Electrostatic Binding in the First-Row AH and A<sub>2</sub> Diatomic Molecules. *Mol. Phys.* **1974**, *27*, 1319–1343.
- (54) Cooper, D. L.; Gerratt, J.; Raimondi, M. The Dipole Moment of LiH (X<sup>1</sup>Σ<sup>+</sup>): Spin-Coupled Valence-Bond Study. *Chem. Phys. Lett.* **1985**, *118*, 580–584.
- (55) Gadéa, F. X.; Leininger, T. Accurate Ab Initio Calculations for LiH and Its Ions, LiH<sup>+</sup> and LiH<sup>-</sup>. *Theor. Chem. Acc.* **2006**, *116*, 566–575.
- (56) Mo, Y.; Zhang, Q. Bonding Features of LiH: A VBSCF Study. *J. Phys. Chem.* **1995**, *99*, 8535–8540.
- (57) Bender, C. F. Correlation Energy and Molecular Properties of Hydrogen Fluoride. *J. Chem. Phys.* **1967**, *47*, 360.
- (58) Bender, C. F. Theoretical Study of Several Electronic States of the Hydrogen Fluoride Molecule. *J. Chem. Phys.* **1968**, *49*, 4989.
- (59) Muenter, J. S. Hyperfine Structure Constants of HF and DF. *J. Chem. Phys.* **1970**, *52*, 6033.
- (60) Lie, G. C. Study of the Theoretical Dipole Moment Function and Infrared Transition Matrix for the X<sup>1</sup>Σ<sup>+</sup> State of the HF Molecule. *J. Chem. Phys.* **1974**, *60*, 2991.
- (61) Krauss, M.; Neumann, D. Multi-Configuration Self-Consistent-Field Calculation of the Dissociation Energy and Electronic Structure of Hydrogen Fluoride. *Mol. Phys.* **1974**, *27*, 917–921.
- (62) Straub, P. A.; McLean, A. D. Electronic Structure of Linear Halogen Compounds. *Theor. Chim. Acta* **1974**, *32*, 227–242.
- (63) Yardley, R. N.; Balint-Kurti, G. G. Ab Initio Valence-Bond Calculations on HF, LiH, LiH<sup>+</sup>, and LiF. *Mol. Phys.* **1976**, *31*, 921–941.
- (64) Tantardini, G. F.; Simonetta, M. Ab Initio Valence Bond Calculations. VII. HF, HF<sup>+</sup>, and H<sub>2</sub>F<sup>+</sup>. *Int. J. Quantum Chem.* **1977**, *12*, 515–525.
- (65) Feller, D.; Peterson, K. A. Hydrogen Fluoride: A Critical Comparison of Theoretical and Experimental Results. *J. Mol. Struct. THEOCHEM* **1997**, *400*, 69–92.
- (66) Scuseria, G. E.; Miller, M. D.; Jensen, F.; Geertsen, J. The Dipole Moment of Carbon Monoxide. *J. Chem. Phys.* **1991**, *94*, 6660.
- (67) Laaksonen, L.; Pyykkö, P.; Sundholm, D. Fully Numerical Hartree–Fock Methods for Molecules. *Comput. Phys. Reports* **1986**, *4*, 313–344.
- (68) Barnes, L. A.; Liu, B.; Lindh, R. Bond Length, Dipole Moment, and Harmonic Frequency of CO. *J. Chem. Phys.* **1993**, *98*, 3972.
- (69) Feller, D.; Boyle, C. M.; Davidson, E. R. One-Electron Properties of Several Small Molecules Using Near Hartree–Fock Limit Basis Sets. *J. Chem. Phys.* **1987**, *86*, 3424.